

# **Analysis and Simulation of Photo Voltaic Cell based Bidirectional Zero Voltage Switching DC-DC Converter Fed Split Phase Induction Motor**

**V. L. N. Sastry<sup>1</sup>, N. Venkata Ramana<sup>2</sup>**

<sup>1</sup>Assistant Professor,  
Sasi Institute of Technology and Engineering,  
Kadakatla, Tadepalligudem,  
West Godavari District, Andhra Pradesh,  
INDIA, 534101.

<sup>2</sup>Assistant Professor,  
Swarnandhra Institute of Engineering and Technology,  
Sitarampuram, Narsapur,  
West Godavari District, Andhra Pradesh,  
INDIA, 534 280.

E-mail: sastry@sasi.ac.in, ramana.navana@gmail.com

**Abstract**—In many industry applications and the real world applications like pump irrigation system, dc motor drives are widely used. In this paper, a novel technique for split phase induction motor drive is discussed to overcome the limited applicability, high cost and maintenance problem of conventional dc motor drives. This technique uses Photo Voltaic (PV) cell, Bidirectional dc-dc converter, a half bridge inverter and a split phase induction motor. The bidirectional dc-dc converter is operated using Zero voltage switching (ZVS), fixed switching frequency and a ripple-free inductor current regardless of direction of power flow. Due to ZVS operation, the reverse recovery problem of the antiparallel diode of the power switch does not occur. It, in turn, reduces the voltage ripple that occurs at the input low voltage source. This paper presents the simulation results of dc-dc converter fed split phase induction motor drive using PV cell.

**Keywords:** Photo Voltaic (PV) cell, Bidirectional dc-dc converter, Zero Voltage Switching (ZVS), Split phase induction motor.

## **1. INTRODUCTION**

Analysis of dc-dc converter fed induction motors are extensively used in the industry applications by replacing the general commutator dc motor. The single phase induction motor is the simplest form of poly phase induction motor having a squirrel cage rotor, except the split phase induction motor that has only one winding on the stator. The split phase induction motor, widely used in utility applications, produces mmf which remains stationary in space and alters with time. The split phase induction motor is usually built with small power for domestic and commercial applications. This paper shows a speed control scheme for split phase induction motor which is fed with a bidirectional dc-dc converter. The conventional nonisolated bidirectional dc-dc converter is shown in Figure 1. The novel bidirectional dc-dc converter is operated with the Zero Voltage Switching as shown in Figure 2. Section 2 gives the literature survey or previous work about the novel bidirectional dc-dc converter along with the modes of operation. Section 3 deals with the modelling of split

phase induction motor where the speed and torque equations are derived. Section 4 emphasizes the proposed drive system with necessary block diagrams. Section 5 deals with the desired simulation results for the proposed drive system. Section 6 gives the conclusion and future scope.

## 2. LITERATURE REVIEW

Bidirectional dc-dc converters have been widely used in various industrial applications such as hybrid electric vehicles, fuel cell vehicles, satellite, and uninterruptable power supplies [1-3]. The bidirectional dc-dc converters are classified as isolated [4] and Nonisolated versions [5]. In both boost and buck modes, the conventional bidirectional dc-dc converter can operate in continuous conduction mode (CCM). The CCM operation can provide a low ripple current. In continuous conduction mode the converter can provide low ripple current. Even though the switching loss of the power switches is high there exists a reverse recovery phenomenon in the power switch. Thus, ZVS operation is achieved.

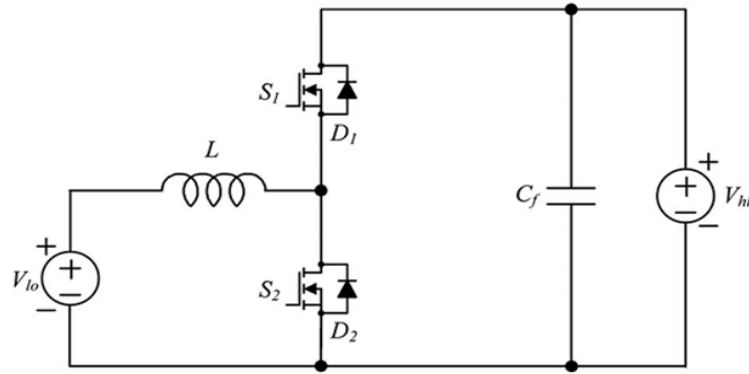


Figure 1: Conventional bidirectional dc-dc converter

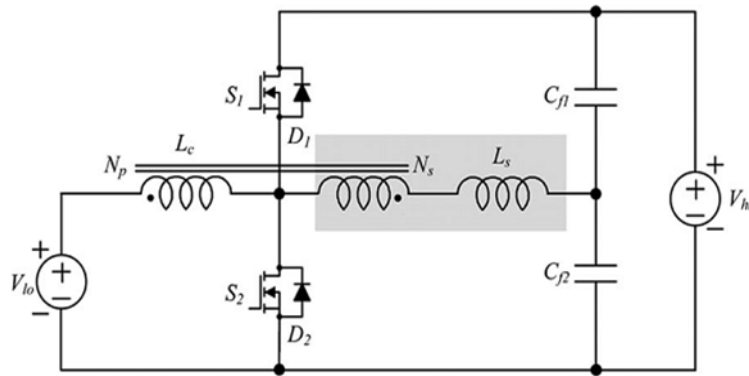


Figure 2: Nonisolated bidirectional ZVS dc-dc converter

A new nonisolated bidirectional ZVS dc-dc converter has a simple auxiliary circuit consisting of an additional winding to the main inductor and an auxiliary inductor which cancels the ripple component of inductor current. The ripple free inductor current can enlarge the lifetime of the battery used as a low side voltage source.

The bidirectional dc-dc converter is shown in Figure 2. It is similar to the conventional converter except additional winding  $N_s$  to the main inductor; auxiliary inductor  $L_s$  is also added. Here existing

filter capacitance  $C_f$  is split into  $C_{f1}$  and  $C_{f2}$  [6].

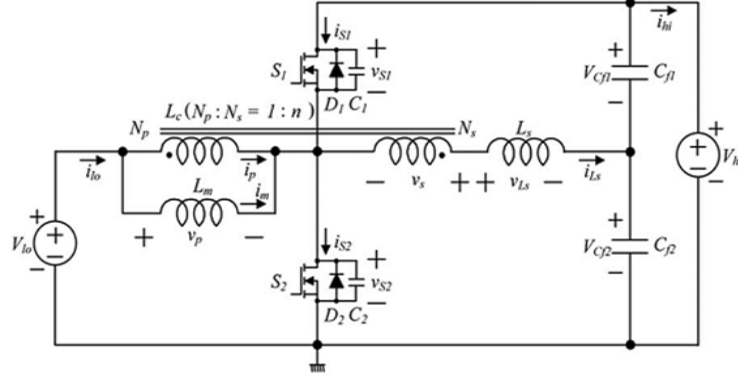


Figure 3: Equivalent circuit of nonisolated bidirectional dc-dc converter

The equivalent circuit of the nonisolated bidirectional dc-dc converter is shown in Figure 3. The coupled inductor  $L_c$  is modelled as a magnetizing inductance  $L_m$  and an ideal transformer has a turn ratio of  $N_p : N_s$  (1:n). The diodes  $D_1$  and  $D_2$  represent the intrinsic diodes of  $S_1$  and  $S_2$ . The capacitors  $C_1$  and  $C_2$  are the parasitic output capacitances of  $S_1$  and  $S_2$ . Since  $C_{f1}$  and  $C_{f2}$  are large they can be treated as dc voltage sources  $V_{Cf1}$  and  $V_{Cf2}$  during the switching period.

- A. Boost mode operation:** Figure 4 shows the theoretical waveforms for the boost mode operation and before  $t_0 S_1$  conducts. The magnetizing current  $I_m$  decreases and the current  $I_{Ls}$  increases linearly. At  $t_0$  they have their minimum and maximum values  $I_{m2}$  and  $I_{Ls1}$  respectively.
- B. Buck mode operation:** The buck operation is similar to the boost operation except that the directions of the magnetizing current  $I_m$  and the low voltage side current  $I_{l0}$  are opposite to those in boost mode. Figure 5 shows waveforms for buck operation and before  $t_0 S_1$  conducts. The magnetizing current  $I_m$  decreases and the current  $I_{Ls}$  increases linearly, and at  $t_0$ , these currents have minimum and maximum values  $-I_{m2}$  and  $I_{Ls1}$  respectively [6].

### 3. MODELLING OF SPLIT PHASE INDUCTION MOTOR

Split phase induction motors are usually constructed with two windings on the stator side and a squirrel cage winding in the rotor side. The auxiliary winding is used to produce a rotating field to start the motor [7]. The axis of the auxiliary winding is placed  $90^\circ$  electrical ahead of the main winding as shown in Figure 6. The simulation of the motor is presented in the stationary d-q frame to facilitate the application of the inverter and the feedback regulators. Because the axis of the main and auxiliary windings is already orthogonal, the stationary d-q axes are chosen aligned with the orthogonal axes of the physical windings. The squirrel cage rotor is represented by equivalent two coils transformed to the stationary d-q axis as shown in Figure 7.

Owing to the presence of two stator windings; namely the main and auxiliary coils and that have different number of turns, they will yield different mutual reactance. Therefore, a transformation is made to transfer the auxiliary winding to an equivalent winding with the same number of turns as that of the main coil. The new variables referred to the equivalent coil are given below [7]:

$$\begin{aligned}
 \Psi_{s\alpha} &= L_{s\alpha} i_{s\alpha} + L_{m\alpha} i_{r\alpha} \\
 \Psi_{s\beta} &= L_{s\beta} i_{s\beta} + L_{m\beta} i_{r\beta} \\
 \Psi_{r\alpha} &= L_{m\alpha} i_{s\alpha} + L_{r\alpha} i_{r\alpha} \\
 \Psi_{r\beta} &= L_{m\beta} i_{s\beta} + L_{r\beta} i_{r\beta}
 \end{aligned} \tag{1}$$

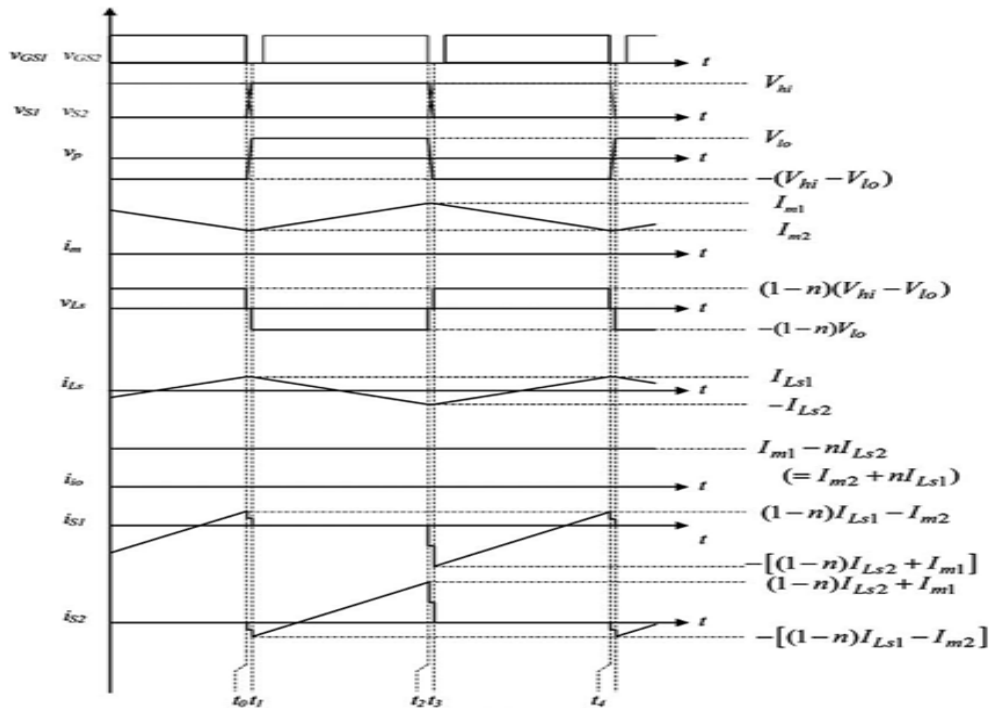


Figure 4: Theoretical waveforms for boost mode [6]

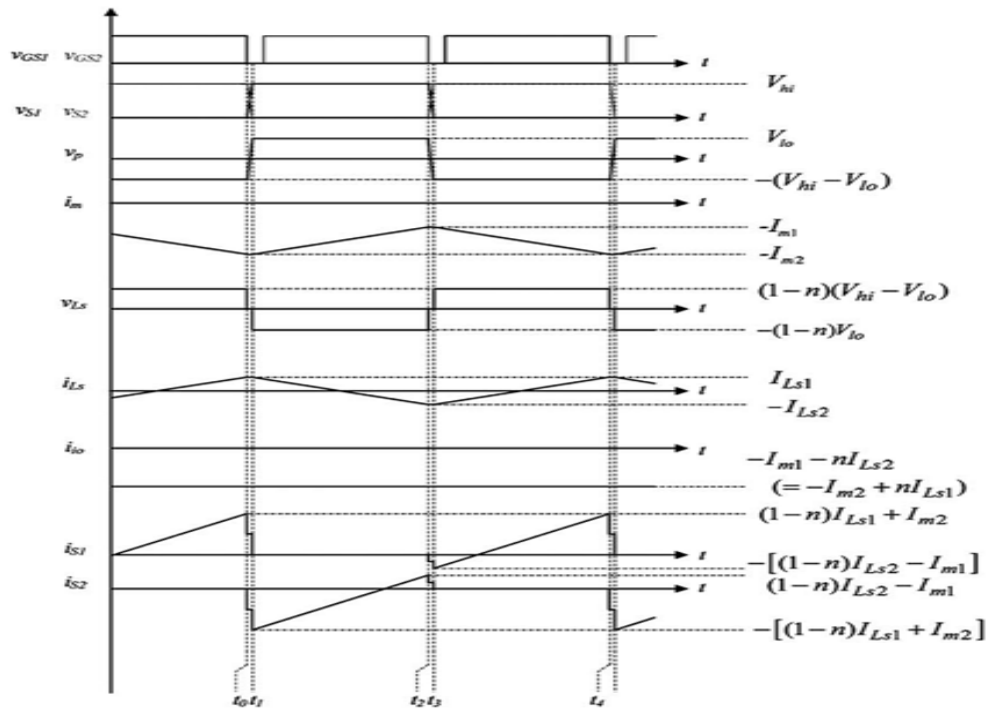


Figure 5: Waveforms for buck mode operation [6]

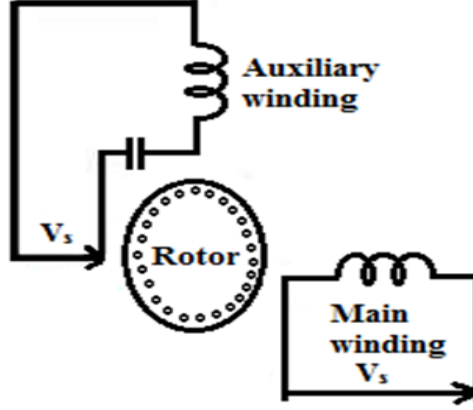


Figure 6: Split phase induction motor

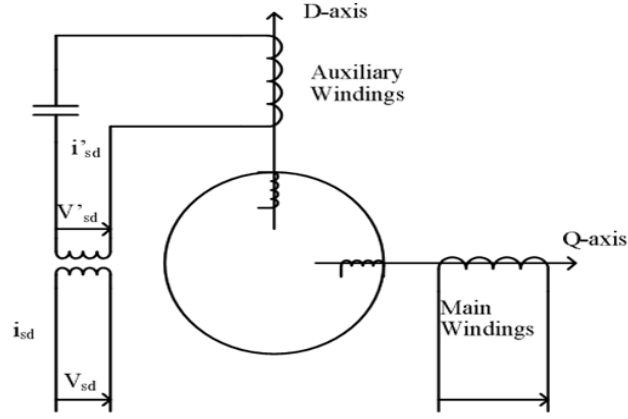


Figure 7: d-q axis transformation of split phase induction motor

The current equation of the motor can be written in the d-q stationary frame as follows:

$$\begin{aligned}
 i_{s\alpha} &= \frac{L_{r\alpha}\Psi_{s\alpha} - L_{m\alpha}\Psi_{r\alpha}}{L_{s\alpha}L_{r\alpha} - L_{m\alpha}^2} \\
 i_{s\beta} &= \frac{L_{r\beta}\Psi_{s\beta} - L_{m\beta}\Psi_{r\beta}}{L_{s\beta}L_{r\beta} - L_{m\beta}^2} \\
 i_{r\alpha} &= \frac{L_{s\alpha}\Psi_{r\alpha} - L_{m\alpha}\Psi_{s\alpha}}{L_{s\alpha}L_{r\alpha} - L_{m\alpha}^2} \\
 i_{r\beta} &= \frac{L_{s\beta}\Psi_{r\beta} - L_{m\beta}\Psi_{s\beta}}{L_{s\beta}L_{r\beta} - L_{m\beta}^2}
 \end{aligned} \tag{2}$$

The equations for torque and speed are given by:

$$\begin{aligned}
 T_e &= P_p(L_{m\beta}i_{s\beta}i_{r\alpha} - L_{m\alpha}i_{s\alpha}i_{r\beta}) \\
 J \frac{d}{dt} \omega_r &= T_e - T_L
 \end{aligned} \tag{3}$$

Here  $\Psi_{s\alpha}, \Psi_{s\beta}, \Psi_{r\alpha}, \Psi_{r\beta}$  are the d-q stator and rotor flux linkage,  $i_{s\alpha}, i_{s\beta}, i_{r\alpha}, i_{r\beta}$  are the stator and rotor currents,  $L_{s\alpha}, L_{s\beta}, L_{r\alpha}, L_{r\beta}$  are the stator and rotor inductances, and  $L_{m\alpha}, L_{m\beta}$  are the

magnetizing inductances, respectively.  $\omega_r$ = rotor speed [electrical rad/sec],  $T_L$ = load Torque,  $J$ = rotor moment of inertia and  $T_e$ = developed Torque.

#### 4. PROPOSED SCHEME

Figure 8 shows the block diagram of proposed drive system which consists of PV cell, ZVS dc-dc converter, Single phase full bridge inverter, and a Split Phase induction motor.

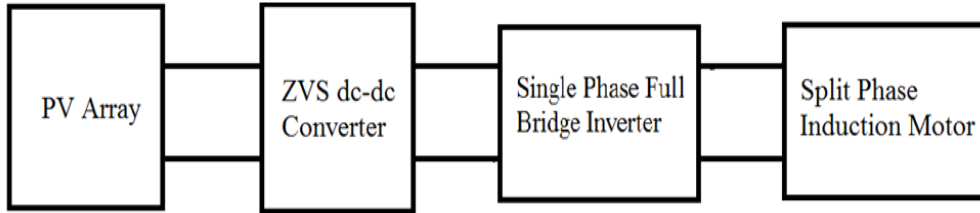


Figure 8: Block diagram of the proposed drive system

##### 4.1. Photo Voltaic (PV) Cell

It is an electrical device which can transform the light energy directly to the electrical energy using photovoltaic effect. When the sunlight or any other light is incident upon a material surface, the electrons present in the valence band absorb energy and, being excited, jump to the conduction band and become free. Some of these free electrons, non-thermal in nature will diffuse, and some of them will reach a junction where they will be accelerated into a different material by a built-in potential [8].

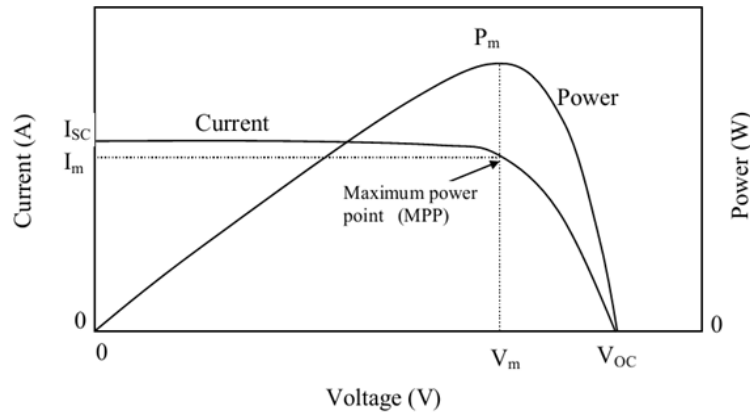


Figure 9: IV characteristics of a Solar Panel

Figure 9 illustrates the I-V curve and power output of a solar panel. If no load is connected with solar panel which is in the sun light, an open circuit voltage  $V_{oc}$  will be produced but no current flows. If the terminals of the solar panel are connected with each other, the short-circuit current  $I_{SC}$  will flow but the output voltage will be zero. In both cases, no power is delivered by the solar panel.

When a load is connected, depending on the I-V curve of the panel and the I-V curve of the load, power can be delivered to the load. The maximum power point (MPP) is the spot near the knee of the I-V curve, and the voltage and current at the MPP are designated as  $V_m$  and  $I_m$ . For

a particular load, the maximum point will change as the I-V curve varies with the temperature, insulation, and shading. As solar power is relatively expensive, it is important to operate panels at their maximum power conditions. In fact dc-dc converters are often used to "match" the load resistance to the Thevenin equivalent resistance of the panel to maximize the power drawn from the panel. These "smart" converters are often referred to as "tracking converters". Specifications of the solar cell used in the proposed drive system is Irradiance = 1000, Temperature = 25 deg,  $V_{oc} = 21.1$  V,  $I_{sc} = 3.8$  Amp,  $I_{mp} = 3.5$  Amp,  $V_{mp} = 17.1$  V.

#### 4.2. ZVS Dc-Dc Converter

The novel nonisolated bidirectional dc-dc converter using Zero Voltage Switching will conduct in two modes i.e., buck and boost. Both the operating modes are similar except the direction of magnetizing current  $I_m$ . This converter connected at the output of the Solar Panel will increase the magnitude of voltage produced by the Solar Panel. The relation between the input and output voltage can be expressed as the following equation.

$$V_{out} = \frac{1}{1-D} V_{in} \quad (4)$$

where  $D = (t_2 - t_1)T_s$ . The time  $(t_2 - t_1)$  is the period of conduction for the switch  $S_2$  in the converter circuit. The specifications of the proposed converter are  $L_m = 155\mu H$ ,  $L_s = 32\mu H$ ,  $C_{f1} = C_{f2} = 3.3\mu F$ . The detailed operation for the proposed converter is given in Section 2 of this paper.

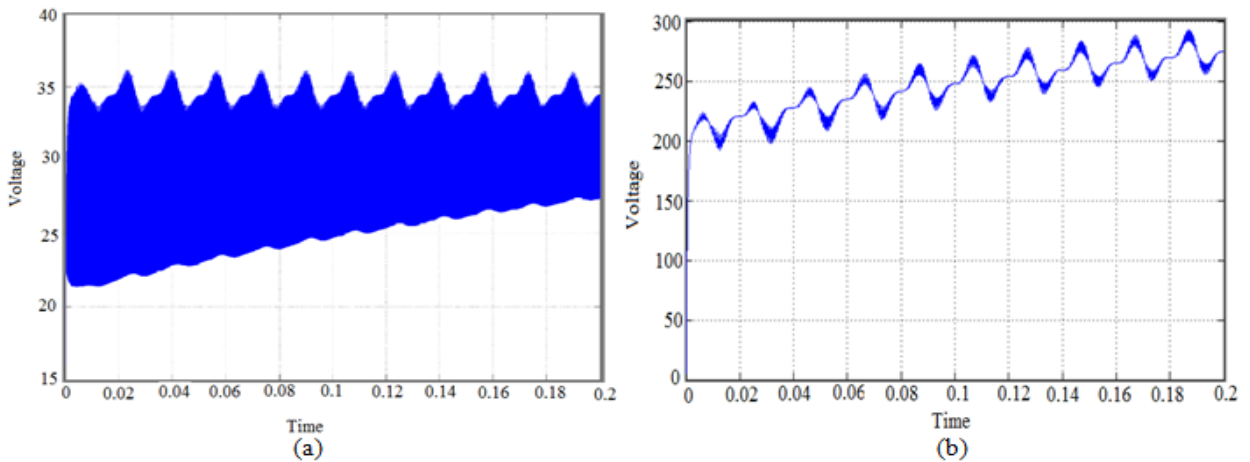


Figure 10: Matlab/Simulink output of the a) PV Cell b) dc-dc Converter

Figure 10(b) shows the output of dc-dc converter when the input is Photo Voltaic array. Because of the unequal voltage of the PV cell given in Figure 10(a) output also oscillatory with increased amplitude. Figures 11 and 12 show the practical wave forms for voltage, current in switch 1, current through inductor  $L_s$  and the current flows in the circuit both in boost mode and buck mode respectively. These wave forms will support the theoretical wave forms presented in Figure 4 and Figure 5.

#### 4.3. Single Phase Full Bridge Inverter

It consists of two arms with a two semiconductor switches on both arms with antiparallel freewheeling diodes for discharging the reverse current. In case of resistive-inductive load, the reverse load current flows through these diodes. These diodes provide an alternate path to inductive current

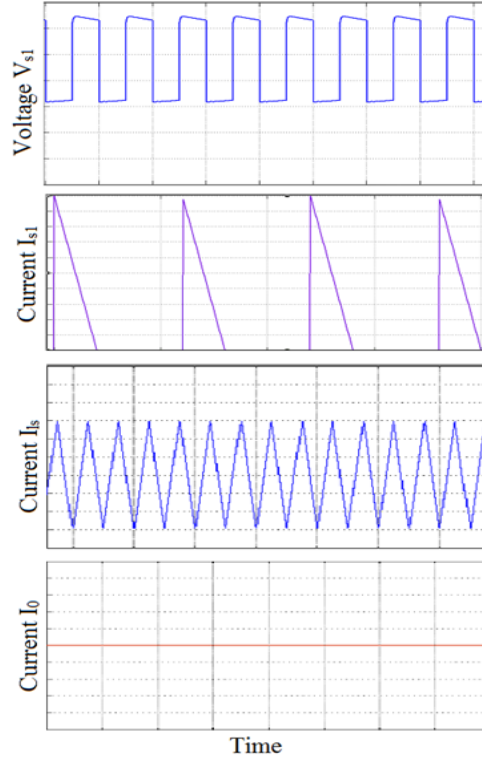


Figure 11: Wave forms in boost mode operation

which continues to flow during the Turn OFF condition. The switching states and the corresponding voltage of the switches used in the two arms of the full bridge inverter are shown in Table 1.

Table 1: Switching States

$T_1$	$T_2$	$T_3$	$T_4$	$V_A$	$V_B$	$V_{AB}$
ON	OFF	OFF	ON	$V_s/2$	$V_s/2$	$V_s$
OFF	ON	ON	OFF	$-V_s/2$	$-V_s/2$	$-V_s$
ON	OFF	ON	OFF	$V_s/2$	$-V_s/2$	0
OFF	ON	OFF	ON	$-V_s/2$	$V_s/2$	0

The switches are  $T_1$ ,  $T_2$ ,  $T_3$  and  $T_4$ . The switches in each branch is operated alternatively so that they are not in same mode (ON /OFF) simultaneously. In practice both are OFF for short period of time known as blanking time, to avoid short circuiting. The switches  $T_1$  and  $T_2$  or  $T_3$  and  $T_4$  should operate in a pair to get the output. These bridge legs are switched such that the output voltage is shifted from one to another and hence the change in polarity occurs in voltage waveform. If the shift angle is zero, the output voltage is also zero and it is maximal when shift

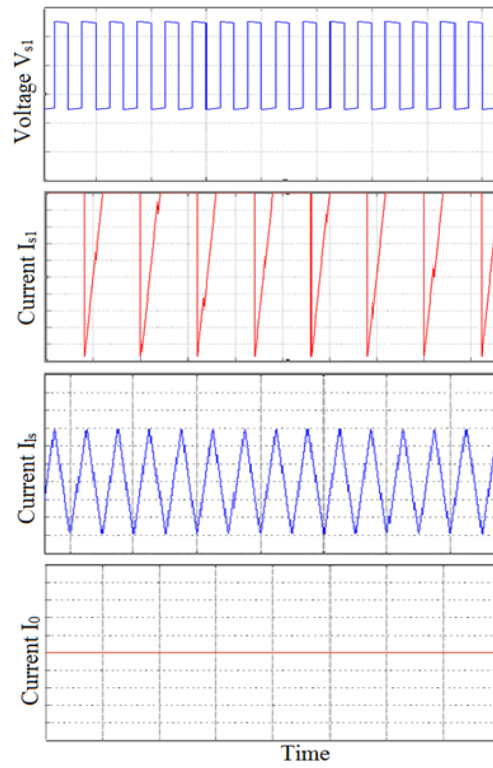


Figure 12: Wave forms in buck mode operation

angle is  $\mu$ . Figure 13 gives the power circuit for a single phase full bridge inverter used to convert the dc output from the ZVS dc-dc converter to an equivalent single phase AC voltage. The voltage obtained is applied to the split phase induction motor.

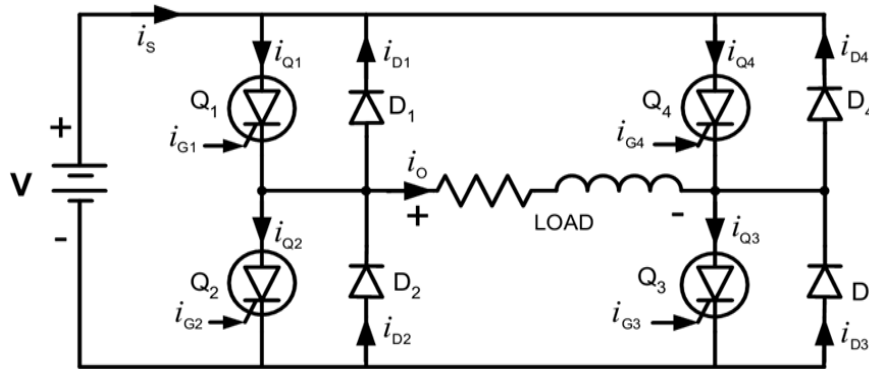


Figure 13: Single Phase Full bridge Inverter

Figure 14 shows the obtained output of the single phase full bridge inverter which is used to convert the dc voltage from the converter to the equivalent ac voltage and fed to the split phase induction motor.

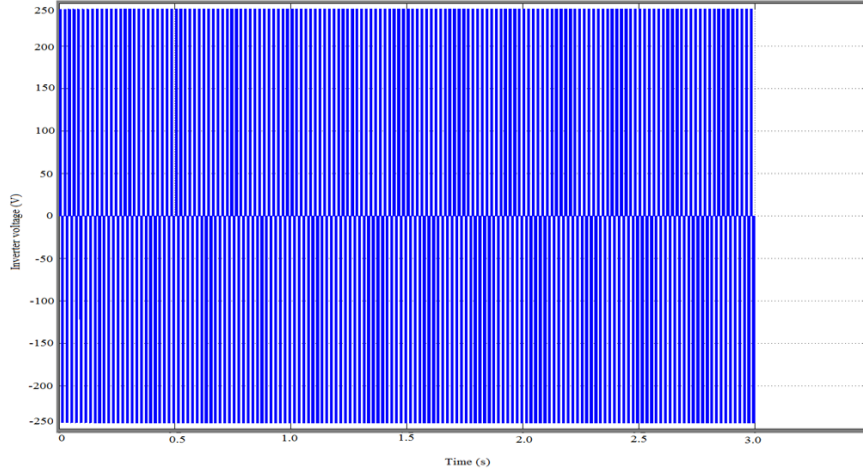


Figure 14: Output Voltage of the Inverter in Matlab Simulink

#### 4.4. Split Phase Induction Motor

The output AC voltage 250 V, 50 Hz obtained from the single phase full bridge inverter, is given to the split phase induction motor which can be operated in different load conditions such as (i) no load (ii) constant load (iii) variable load. The modelling of the voltage, current and torque equations of the split phase induction motor are presented in Section 3 of this paper. The specifications used for the motor are as follows:

Nominal Power = 0.25 Hp Voltage = 250 V, Frequency = 50 Hz.

Resistance of Main winding Stator  $R_s = 2.02$  ohm, Leakage Inductance  $L_{ls} = 7.4$  mH.

Resistance of Main winding Rotor  $R_{r'} = 4.12$  ohm, Leakage Inductance  $L_{lr'} = 5.6$  mH.

Mutual inductance of main winding  $L_{ms} = 0.1772$  H

Resistance of Auxiliary winding stator  $R_s = 7.14$  ohm, Leakage Inductance  $L_{ls} = 8.5$  mH.

### 5. SIMULATION RESULTS

This section deals with the MATLAB/Simulink Model for the proposed drive system, and their results with different load conditions specified in Section 4.4. All the simulations are done at a moment of inertia  $J = 0.00146$  kg-m<sup>2</sup> and viscous friction coefficient  $D_f = 0$  Nm-s.

The dynamic behaviour of motor supplied by 250 V and 50 Hz is studied under the following conditions:

- 1 Starting the motor with no-load until steady state reaches.
- 2 Starting the motor at a constant Load as  $T_L = 0.1$  N-m until steady state reached.
- 3 Starting the motor with a load of  $T_L = 1.5$  N-m and at time  $t = 1$  sec the load will decrease to its constant value  $T_L = 0.1$  N-m until steady state reached.

Figure 15 shows the complete Simulink model for the proposed system consisting of PV cell, ZVS dc-dc converter, single phase Inverter and a Split phase Induction motor.

Figures 16-19 give the Matlab/Simulink results of main winding current, Speed-Torque curve, Electromagnetic Torque and Rotor speed respectively when (i) No load is applied and (ii) Constant Load of  $T_L = 0.1$  N-m is applied to the Split Phase Induction motor. Here for the two cases No load and Constant Load Split Phase Induction motor will produce same response.

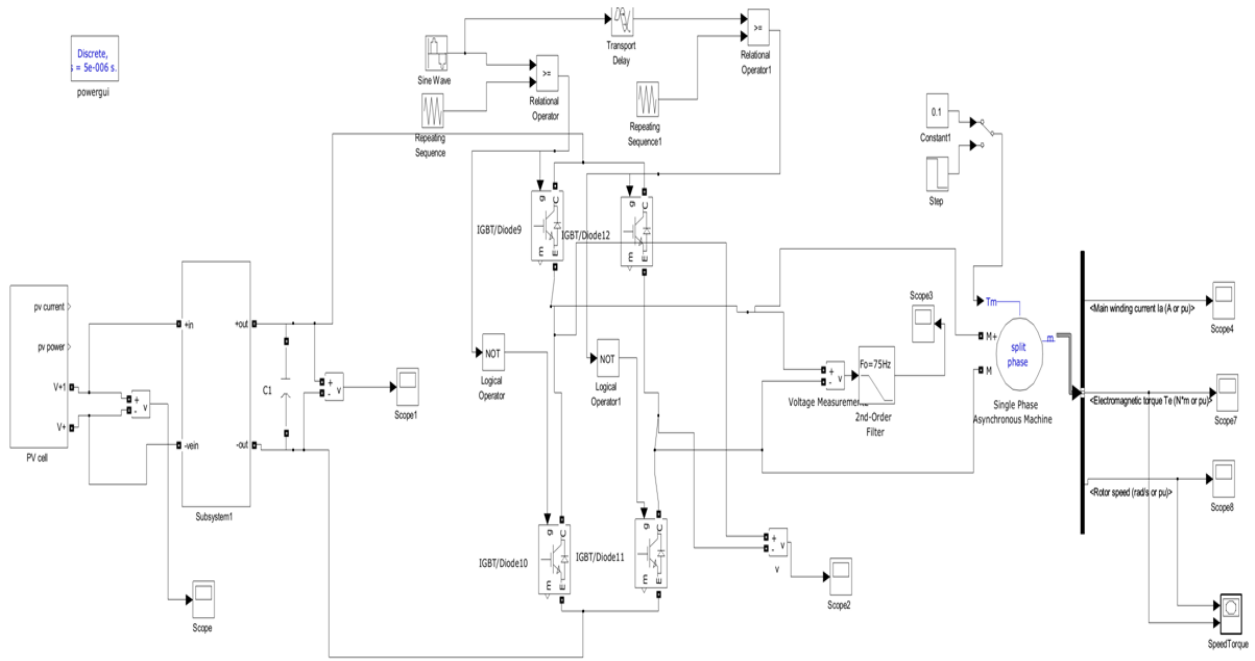


Figure 15: MATLAB/Simulink model for the proposed system

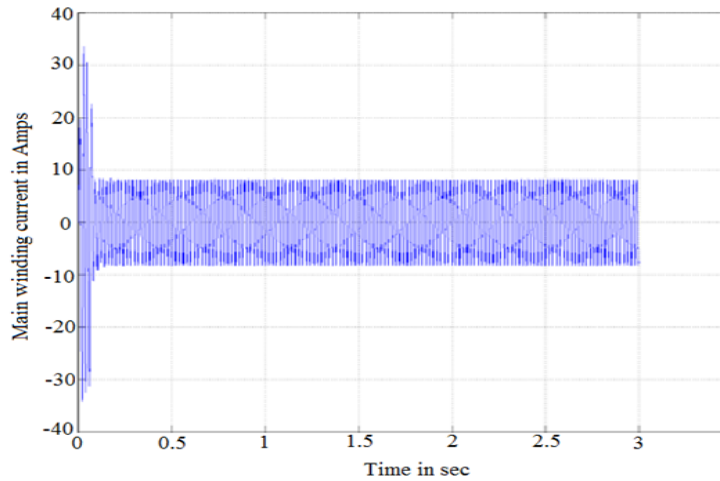


Figure 16: Main winding current

Figures 20-23 give the Matlab Simulink results of main winding current, Speed-Torque curve, Electromagnetic Torque and Rotor speed respectively when (iii) Load torque  $T_L$  is changed from 1.5 N-m to 0.1 N-m at time  $t = 1$  sec. In this condition the Main winding current slightly decreases and the Rotor Speed will increase when the Torque is changed from 1.5 N-m to 0.1 N-m at time  $t = 1$  second.

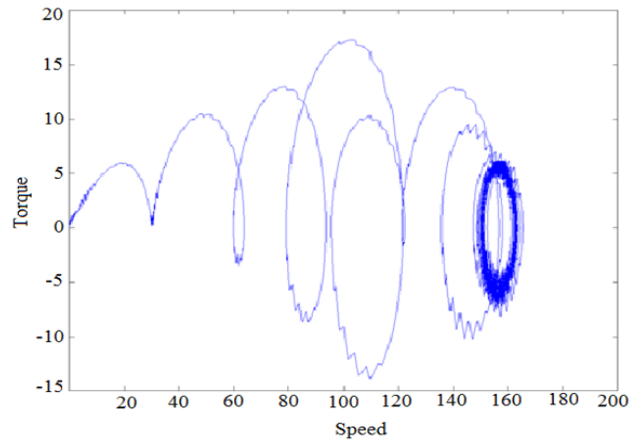


Figure 17: Speed-Torque curve

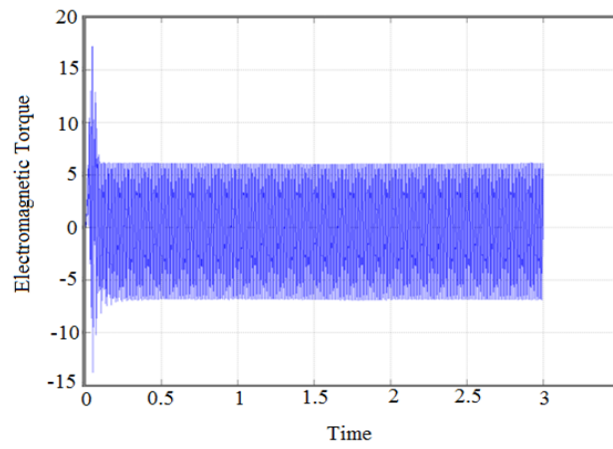


Figure 18: Electromagnetic Torque

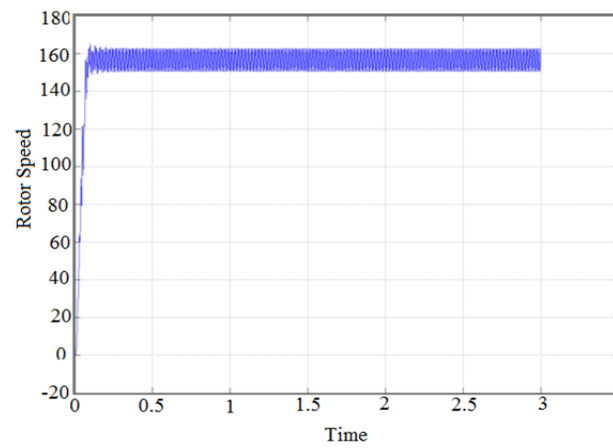


Figure 19: Rotor Speed

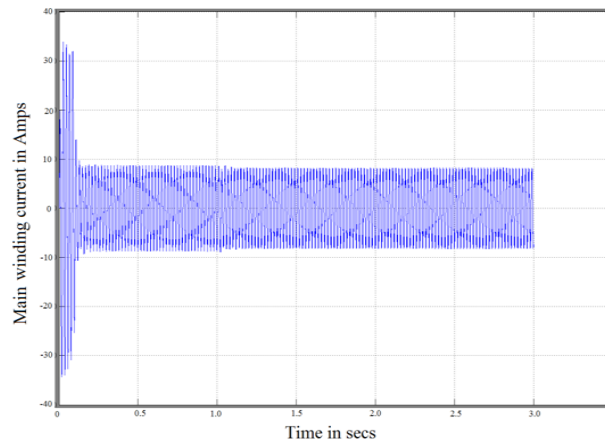


Figure 20: Main winding current

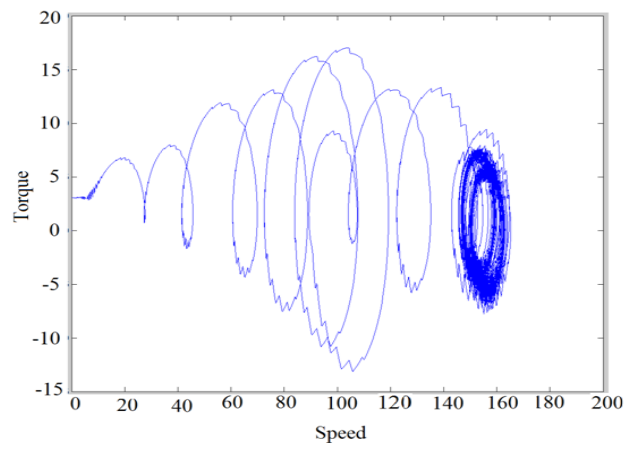


Figure 21: Speed-Torque curve

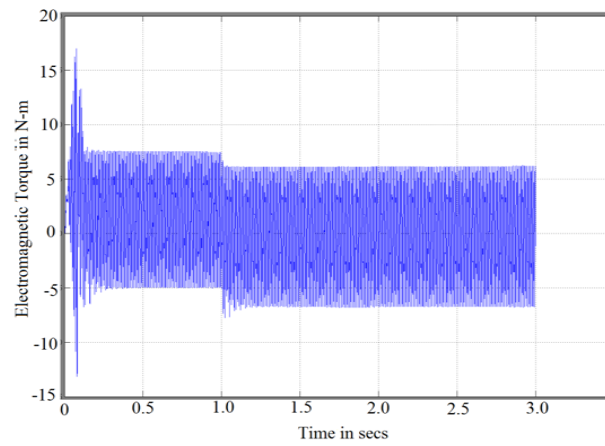


Figure 22: Electromagnetic Torque

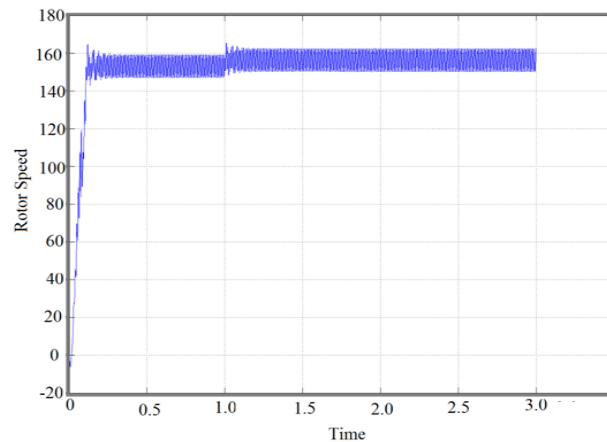


Figure 23: Rotor Speed

## 6. CONCLUSION

This paper presents the analysis and simulation performance of a proposed drive system for various loads conditions and the results are presented in Section 5. It also proves that the ZVS dc-dc converter is a better solution for the reverse recovery of the antiparallel diodes in the case of split phase induction motor drives. Further this paper can be implemented in hardware like FPGA and DSP for real time applications. This paper can also be extended in terms of *Thermal* and *FEM* analysis of the machine for various load conditions using softwares like JMAG, MAXWELL.

## REFERENCES

1. Tao, H., Duarte, J. L. and Handrix, M. A. M. 2008. Line-Interactive UPS using a Fuel Cell as the Primary Source. *IEEE Trans. Ind. Electron.*, vol. 55(8):3012-3021.
2. Chen, L. R., Chu, N. Y., Wang, C. S. and Liang, R. H. 2008. Design of a Reflex-Based Bidirectional Converter with the Energy Recovery Function. *IEEE Trans. Ind. Electron.*, vol. 55(8):3022-3029.
3. Shang, F. and Yan, Y. 2009. Novel Forward-Flyback Hybrid Bidirectional Dc-Dc Converter. *IEEE Trans. Ind. Electron.*, vol. 56(5):1578-1584.
4. Wu, T. F., Chen, Y. C., Yang, J. G. and Kuo, C. L. 2010. Isolated Bidirectional Full-Bridge Dc-Dc Converter with a Flyback Snubber. *IEEE Trans. Power Electron.*, vol. 25(7):1915-1922.
5. Das, P., Mousavi, S. A. and Moschopoulos, G. 2010. Anaysis and Design of a Nonisolated Bidirectional ZVS-PWM Dc-Dc Converter with Coupled Inductor. *IEEE Trans. Power Electron.*, vol. 25(10):2630-2641.
6. Do, H-L. 2011. Nonisolated Bidirectional Zero-Voltage-Switching Dc-Dc Converter. *IEEE Trans. Power Electronics*, vol. 26(9)P:2563-2569.
7. Singh, A. P. and Giri, V. K. 2012. Modelling and Simulation of Single Phase Cycloconverter. *International Journal of Engineering Science and Technology*, Vol. 2(2):346-351.
8. Hilloowala, R. M. and Sharaf, A. M. 1990. Single Phase Induction Motor Drive Scheme for Pump Irrigation using Photovoltaic Source. (IEEE 1990).